

# A COMPARISON OF SENTINEL-2A AND SENTINEL-2B WITH PRELIMINARY RESULTS

Feng Chen<sup>1</sup>, Cheng Ming<sup>1</sup>, Jonathan Li<sup>1,2</sup>, Cheng Wang<sup>1</sup>, Martin Claverie<sup>3</sup>

<sup>1</sup> Fujian Key Laboratory of Sensing and Computing for Smart Cities, Xiamen University, Xiamen, China

<sup>2</sup> Department of Geography and Environmental Management, University of Waterloo, Waterloo, Canada

<sup>3</sup> University of Maryland, Department of Geographical Sciences, College Park, MD, USA

## ABSTRACT

Currently, two Sentinel-2 satellites (Sentinel-2A and Sentinel-2B) have been operated simultaneously, since the launch of Sentinel-2B on 7 March 2017. The Multi-Spectral Instrument (MSI) onboard each platform is identically designed. However, as indicated by spectral response function (SRF), there is channel difference (more or less) between two MSIs. An investigation to show comparison of Sentinel-2A and Sentinel-2B in terms of channel reflectance and derived spectral index was conducted accordingly. The preliminary results mainly based on ASTER Spectral Library Version 2.0 are shown. Findings are included: (1) channel reflectance of Sentinel-2A MSI is averagely greater than channel reflectance of Sentinel-2B MSI over most channels; (2) the difference in channel reflectance is more significant for B1 (Costal Aerosol), B2 (Blue), and B12 (SWIR); (3) the difference in derived spectral index (i.e., NDVI) is more significant, compared with the difference in reflectance of individual channels correspondingly. To ensure the product consistency between two MSIs, investigations based on more spectra collections and actual observation pairs should be done further.

**Index Terms**—Reflectance, Multi-Spectral Instrument (MSI), Spectral response function (SRF), Consistency, Spectra library, Hyperion

## 1. INTRODUCTION

Currently, two Sentinel-2 satellites (Sentinel-2A and Sentinel-2B) with an identically designed sensor—the Multi-Spectral Instrument (MSI), have been operated simultaneously, phased at 180° to each other. Sentinel-2A was launched on 23 June 2015, while Sentinel-2B satellite was launched on 7 March 2017. When two sensors are operated simultaneously, the mission's revisit time is about 5 days, while about 10 days with one satellite in operation. In addition, with its 13 spectral channels (Fig. 1), from the visible and the near-infrared (VNIR) to the shortwave infrared (SWIR) with suitable spatial resolutions (ranging from 10 m to 60 m), the MSI onboard Sentinel-2 makes global land monitoring to an unprecedented level (<https://earth.esa.int/web/sentinel/missions/sentinel-2>). As shown in Fig. 1, there is still difference (more or less) in

channel settings between two MSI sensors. The channel associated difference may challenge between-sensor consistency in observation and retrieved variables.

Spectral response function (SRF) was taken as an important aspect of the channel settings, as discussed previously [3], [5]. Effects of the difference in SRF on corresponding values between two Sentinel-2 MSIs (Fig. 1) were investigated, including channel reflectance and derived spectral index. Spectra samples separately from ASTER Spectral Library Version 2.0 and Hyperion data archives were used in obtaining the channel reflectance. Descriptions on channel reflectance calculation are detailed in Section 2. However, results based on ASTER Spectral Library Version 2.0 are mainly shown in this paper, due to the space limit.

## 2. DATA AND METHODS

Channel reflectance over a specific channel is an average value of spectra reflectance weighted by SRF, which is obtained through a normalized integration (Eq. (1)).

$$\text{Ref}_{\text{Bi}} = \frac{\int_{\lambda_s}^{\lambda_e} \text{SRF}_{\text{Bi}}(\lambda) \text{Ref}(\lambda) d\lambda}{\int_{\lambda_s}^{\lambda_e} \text{SRF}_{\text{Bi}}(\lambda) d\lambda} \quad (1)$$

where  $\text{SRF}_{\text{Bi}}(\lambda)$  is the SRF of a specific channel Bi, which is given with discrete pattern and finite range, while  $\lambda_s$  and  $\lambda_e$  are the start wavelength and the end wavelength of channel Bi.  $\text{Ref}(\lambda)$  is the reflectance at a specific wavelength  $\lambda$ .

The SRFs (Version 2.0) of Sentinel-2 A/B MSI were obtained from <https://earth.esa.int/web/sentinel> (assessed on 1 December 2017).

### 2.1. Channel reflectance based on spectra in ASTER Spectral Library Version 2.0

ASTER Spectral Library Version 2.0 contains over 2300 spectra, providing one of the most comprehensive collections of spectra covering the wavelength from the visible to thermal infrared region [1]. The spectra in ASTER Spectral Library Version 2.0 are available from <http://speclib.jpl.nasa.gov>. Difference in wavelength range between the SRFs of Sentinel-2A/B MSI and the spectra

may result in bias in channel reflectance calculation (Eq. (1)).

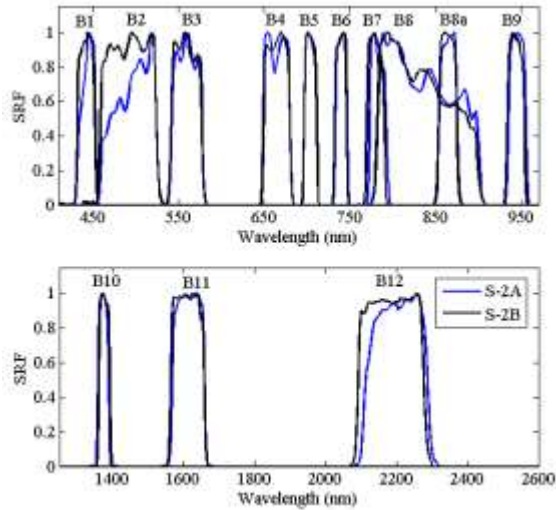


Fig. 1. Spectral response functions (SRFs) of the MSI, onboard Sentinel-2A (blue line) and Sentinel-2B (black line) over the visible and near infrared (VNIR) regions (up) and the short-wave infrared (SWIR) regions (below).

Accordingly, the spectra of which the wavelength covers the spectral range of all MSI channels (420-2400 nm) were selected. A spectra sample named “Trona Na<sub>3</sub>(CO)(HCO<sub>3</sub>)\*2H<sub>2</sub>O” was excluded, due to its reflectance recorded greater than 1.0. Totally, 406 spectra selected from ASTER Spectral Library Version 2.0 were used. In addition, difference in spectral resolution between the spectra and the SRFs of MSI was tackled properly through an interpolation procedure [3].

## 2.2. Channel reflectance based on Hyperion spectra

Details on the SRF of Hyperion are not publicly accessible. However, for a specific channel  $i$  of Hyperion, the SRF expressed as  $R_i^H(\lambda)$  is modeled, based on the full width at half maximum (FWHM) and center wavelength (Eq. (2)).

$$SRF_i^H(\lambda) = \exp\left(-\frac{4\ln(2)(\lambda - \lambda_{ic})^2}{(FWHM_i)^2}\right) \quad (2)$$

where  $FWHM_i$  is the FWHM of channel  $i$ , while  $\lambda_{ic}$  is the center wavelength of channel  $i$ . The superscript “H” stands for Hyperion.

The Hyperion instrument provides a high resolution hyperspectral imager which is capable of resolving 220 unique spectral channels (400~2500 nm). Each channel is provided with averagely 10 nm FWHM and with a spatial resolution of 30 m. The Level 1 radiometric product has a total of 242 channels, but only 198 channels are calibrated. In addition, due to an overlap between the VNIR and SWIR focal planes, there are actually only 196 unique channels.

The center wavelength and the FWHM of all calibrated bands of Hyperion from the website (<https://eo1.usgs.gov/sensors/hyperioncoverage>) were used in getting the SRFs.

Three procedures were used to get the channel reflectance for Sentinel-2A/B MSI correspondingly based on the calibrated Hyperion spectra, including weights calibration (Eq. (3)), weights normalization (Eq. (4)), and weighted sum as reflectance integration (Eq. (5)).

$$W_i^H = \int_{\lambda_{is}}^{\lambda_{ie}} SRF_i^H(\lambda) SRF^{S2}(\lambda) d\lambda \quad (3)$$

$$nW_i^H = \frac{W_i^H}{\sum_i W_i^H} \quad (4)$$

$$Ref_{Bi}^{S2} = \sum_i (nW_i^H \times Ref_i^H) \quad \text{with } (\lambda_{ic}^H \in (\lambda_{Bis}^{S2}, \lambda_{Bie}^{S2})) \quad (5)$$

where  $W_i^H$  and  $nW_i^H$  are weight and normalized weight for Hyperion channel  $i$ , respectively.  $Ref_{Bi}^{S2}$  is the reflectance of MSI channel  $Bi$ , which is an integration of all valid Hyperion channels with the center wavelength ( $\lambda_{ic}^H$ ) being located within  $(\lambda_{Bis}^{S2}, \lambda_{Bie}^{S2})$ . By the way,  $\lambda_{Bis}^{S2}$  and  $\lambda_{Bie}^{S2}$  are the start wavelength and the end wavelength of MSI channel  $Bi$ . The superscript “S2” stands for Sentinel-2.

## 2.3. Measures for difference

To show generally overall measures of the difference in channel reflectance between Sentinel-2A and -2B, three indicators were used, including the mean difference (MD), the root mean square deviation (RMSD), and the mean relative difference (MRD). Actually, the indicators were used previously [2].

$$MD_{Bi} = \text{mean}(Ref_{jBi}^{S2A} - Ref_{jBi}^{S2B}) \quad (6)$$

$$RMSD_{Bi} = \text{sqrt}(\text{mean}((Ref_{jBi}^{S2A} - Ref_{jBi}^{S2B})^2)) \quad (7)$$

$$MRD_{Bi} = \text{mean}\left(2 \times \frac{(Ref_{jBi}^{S2A} - Ref_{jBi}^{S2B})}{(Ref_{jBi}^{S2A} + Ref_{jBi}^{S2B})} \times 100\right) \quad (8)$$

where  $Ref_{jBi}^{S2A}$  and  $Ref_{jBi}^{S2B}$  are reflectance values (for spectra  $j$ ) of MSI channel  $Bi$  for Sentinel-2A and -2B respectively, while  $\text{mean}()$  and  $\text{sqrt}()$  are procedures for obtaining the mean value and square root value respectively. The Eq. (9) measures individual (for spectra  $j$ ) relative difference between the corresponding values of two MSIs.

$$RD_{Bi} = 2 \times \frac{(Ref_{jBi}^{S2A} - Ref_{jBi}^{S2B})}{(Ref_{jBi}^{S2A} + Ref_{jBi}^{S2B})} \times 100 \quad (9)$$

## 2.4. Comparison of the derived spectral index

Normalized Difference Vegetation Index (NDVI) has been used as a measure to characterize landscape and to model

urban thermal environment. In this investigation, the NDVI of Sentinel-2A/B MSI data was calculated through Eq. (10), according to the descriptions shown at the official web (<https://sentinel.esa.int/web/sentinel/technicalguides/sentinel-2-msi/level-2a/algorithm>).

$$NDVI^{S2} = \frac{(Ref_{B8}^{S2} - Ref_{B4}^{S2})}{(Ref_{B8}^{S2} + Ref_{B4}^{S2})} \quad (10)$$

### 3. RESULTS

Generally, the RMSD of channel reflectance between two MSIs is more significant for B1, B2, B3, B7, and B12, according to the ASTER spectra selections. The MD shows that the channel reflectance of Sentinel-2A is averagely greater than the channel reflectance of Sentinel-2B over most channels. The MRD is relatively obvious for B1, B2, B3, and B12, while is minor for B5, B8, and B8a (Table 1). The significant difference in SRF (Fig. 1) may largely contribute to the relatively obvious deviation in channel reflectance over individual channels (i.e., B1, B2, and B12).

Comparable findings are obtained through the ASTER spectra selections and the Hyperion spectra collections separately, although individual measures are different more or less (Table 1). For example, considering the MRD, between-sensor differences are obvious in B1, B2, B6, and B7, whereas are minor in B4, B5, B8, and B8a. By the way, statistics for B9 and B10 are not included in Table 1, due mainly to possible effects on Hyperion data related to atmospheric water vapor absorption over these channels.

Table 1 Differences in channel reflectance based on ASTER spectra selections (406) and Hyperion spectra collections (10, 000)

	ASTER spectra selections			Hyperion		
	MD	RMSD	MRD	MD	RMSD	MRD
B1	0.088	0.124	0.552	-0.105	0.144	-3.076
B2	0.193	0.278	0.945	0.253	0.278	3.841
B3	0.049	0.095	0.220	0.031	0.058	0.237
B4	-0.010	0.019	-0.032	0.010	0.015	0.128
B5	0.002	0.005	0.007	0.006	0.009	0.060
B6	0.026	0.086	0.097	0.345	0.407	1.542
B7	0.033	0.124	0.091	-0.310	0.410	-1.180
B8	-0.002	0.053	-0.009	0.040	0.059	0.160
B8a	-0.001	0.024	-0.007	-0.034	0.044	-0.127
B11	0.035	0.081	0.098	0.119	0.130	0.571
B12	-0.285	0.647	-0.732	-0.133	0.277	-0.341

(Note: Values of MD and RMSD in this table are scaled with 100).

Details on relative difference are demonstrated through a scatter plot (Fig. 2). For most channels, the relative differences of all spectra samples are within 1%, especially for B4, B5, B8, and B8a. For B1, B2, and B12, many samples showing significant difference (greater than 5%) are observed, most of which are located in low reflectance (less than 0.5). A non-parametric correlation test called “Kendall” rank test was used to investigate the relationship between the relative difference and actual channel reflectance (of

Sentinel-2A). The test results show that no significant relationship is observed between the relative difference and actual reflectance ( $P > 0.05$ ) for most MSI channels, except two SWIR channels (B11 and B12). The randomness of the relative difference suggests that linear transformation model used to eliminate or decrease the between-sensor differences may not be effective for most channels, as shown in Fig. 2. However, findings based on Hyperion spectra collections are not completely consistent with those given in Fig. 2, which are not shown because of space limit of the manuscript.

Totally, 288 samples of the ASTER spectra selections with NDVI values greater than 0, are presented in Fig. 3. Relative differences in the individual channels (i.e., B4 and B8) and the difference in corresponding spectral index (i.e., NDVI) are shown in Fig. 3. The ranges of relative difference in NDVI are values at the [5%, 95%] of cumulative distribution. In particular, for samples from the ASTER spectra selections, the values are approximate to -6% and 5% (Fig. 3). Relative difference in NDVI for spectra with low NDVI value is likely more significant. However, the relationship between the relative difference and actual NDVI is not linearly significant (Fig. 3(a)). Furthermore, Fig. 3(b) shows the contributions of two individual channels (i.e., B4 and B8) to final relative difference in NDVI.

### 4. DISCUSSION AND CONCLUSIONS

The measured SRFs (Version 2) of MSIs show difference between two Sentinel-2 satellites (Sentinel-2A and Sentinel-2B). The difference is especially demonstrated for B1, B2, and B12, although the two MSIs were designed identically. Consequently, the difference in the SRF largely contributes to the relatively obvious deviation in the channel reflectance for B1, B2, and B12, between two MSIs.

Compared with the differences in reflectance of individual channels, the difference in derived spectral index (i.e., NDVI) is more significant. Specifically, as shown in Fig. 2, minor differences in the channel reflectance are recorded for both B4 and B8, which are less than 1%, while the difference in NDVI is greater than 1% for most spectra samples (Fig. 3). Furthermore, findings on the relative difference suggest that linear transformation model used to eliminate or decrease the difference in channel reflectance between Sentinel-2A and Sentinel-2B may not be effective for most channels and for the derived spectral index.

Difference in spectra samples (e.g., classes and number) and discrepancy in spectra characteristics (e.g., spectral resolution and uncertainty) between the ASTER spectra selections and Hyperion spectra collections may contribute to possible bias in results and conclusions. Accordingly, further investigations based on more other spectra collections should be done, as done by [4]. The actual SRFs of Sentinel-2 MSIs are based on ground measurements performed in the frame of the Assembly, Integration and Test campaign (in metadata). The actual SRFs may change

more or less during the satellite operation in orbit, which are required to be updated regularly. Thereby, for practical

needs, actual observation pairs of Sentinel-2A and -2B are necessarily to be collected for investigations further.

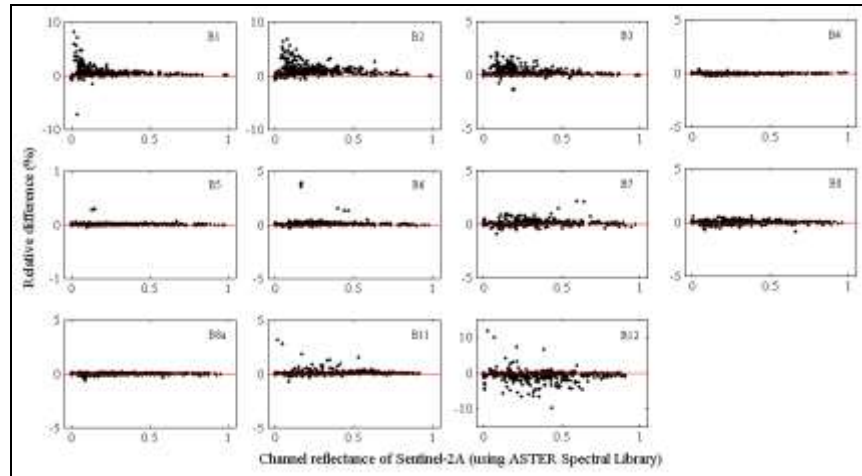


Fig. 2. Relative difference in channel reflectance between Sentinel-2A and Sentinel-2B, using 406 spectra from ASTER Spectral Library Version 2.0. Relative difference in this figure is defined as Eq. (9).

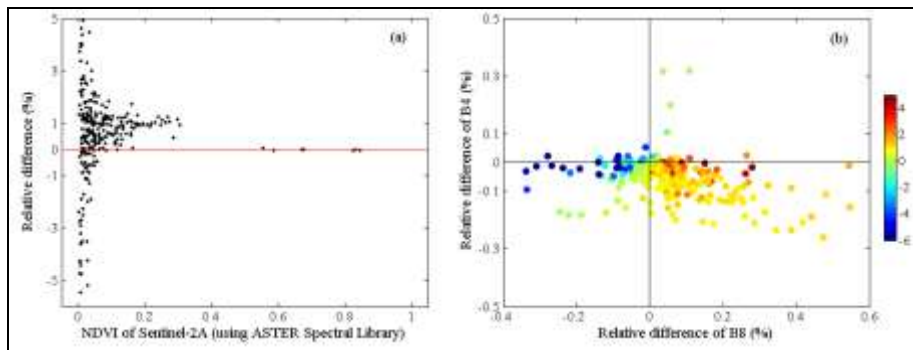


Fig. 3. Demonstrations for (a) Relative difference of NDVI and (b) comparison of individual channel reflectance and NDVI, using 406 spectra from ASTER Spectral Library Version 2.0.

## 5. ACKNOWLEDGEMENTS

This research was jointly supported by the National Key Research and Development Program of China (Grant 2016YFC1401001 and 2016YFC1401008), China Postdoctoral Science Foundation (Grant 2017M612124), and National Natural Science Foundation of China (Grant U1605254). Appreciations are given to Dr. Simon Hook at NASA JPL, for the provision of ASTER Spectral Library Version 2.0. We acknowledge Prof. Su Z. (Bob) of University of Twente and Prof. Qihao Weng of Indiana State University, for their valuable suggestions during this investigation.

## 6. REFERENCES

- [1] A.M. Baldridge, S.J. Hook, C.I. Grove, and G. Rivera, "The ASTER spectral library version 2.0," *Remote Sens. Environ.*, Elsevier, New York, USA, vol. 113, pp. 711-715, 2009.
- [2] D.P. Roy, V. Kovalsky, H.K. Zhang, E.F. Vermote, L. Yan, S.S. Kumar, and A. Egorov, "Characterization of Landsat-7 to Landsat-8 reflective wavelength and normalized difference vegetation index continuity," *Remote Sens. Environ.*, Elsevier, New York, USA, vol. 185, pp. 57-70, 2016.
- [3] F. Chen, S. Yang, Z. Su, and K. Wang, "Effect of emissivity uncertainty on surface temperature retrieval over urban areas: Investigations based on spectral libraries," *ISPRS J. Photogramm.*, Elsevier, Amsterdam, Netherlands, vol. 114, pp. 53-65, 2016.
- [4] J. Gorroño, A.C. Banks, N.P. Fox, and C. Underwood, "Radiometric inter-sensor cross-calibration uncertainty using a traceable high accuracy reference hyperspectral imager," *ISPRS J. Photogramm.*, Elsevier, Amsterdam, Netherlands, vol. 130, pp.393-417, 2017.
- [5] G. Chander, N. Mishra, D.L. Helder, D.B. Aaron, A. Angal, T. Choi, X. Xiong, and D.R. Doelling, "Applications of spectral band adjustment factors (SBAF) for cross-calibration," *IEEE T. Geosci. Remote.*, Piscataway, USA, vol. 51(3), pp.1267-1281, 2013.